Molecular Cell, Volume *60*

## Supplemental Information

# Continuous Histone Replacement by Hira Is Essential for Normal Transcriptional Regulation and De Novo DNA Methylation during Mouse Oogenesis

Buhe Nashun, Peter W.S. Hill, Sebastien A. Smallwood, Gopuraja Dharmalingam, Rachel Amouroux, Stephen J. Clark, Vineet Sharma, Elodie Ndjetehe, Pawel Pelczar, Richard J. Festenstein, Gavin Kelsey, and Petra Hajkova

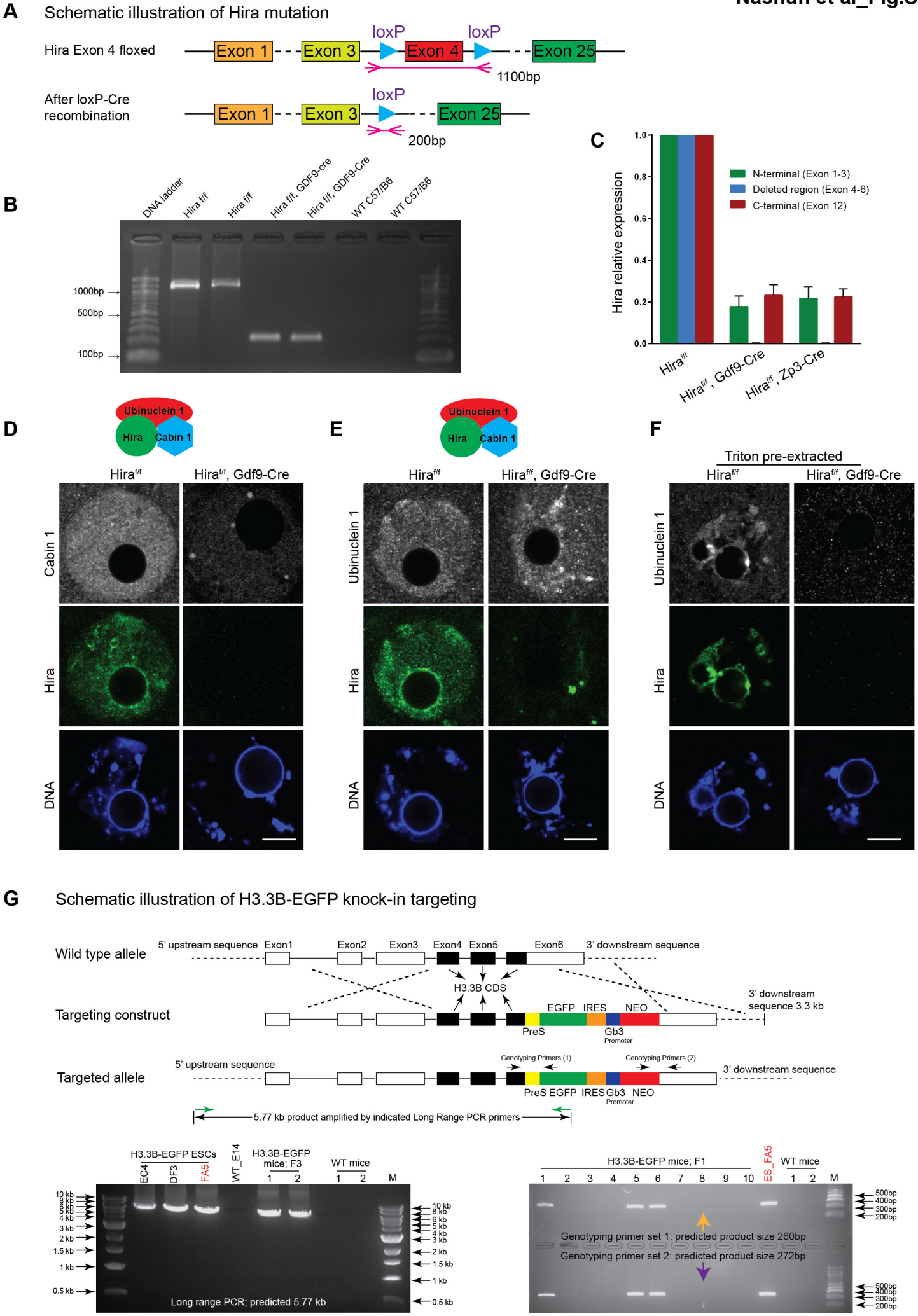
A
Schematic illustration of Hira mutation
Hira Exon 4 floxed
Exon 1
Exon 3
loxP
Exon 4
loxP
Exon 25
1100bp
After loxP-Cre recombination
Exon 1
Exon 3
loxP
Exon 25
200bp
B
DNA ladder
Hira f/f
Hira f/f
Hira f/f, GDF9-cre
Hira f/f, GDF9-Cre
WT C57/B6
WT C57/B6
1000bp
500bp
100bp
C
Hira relative expression
1.0
0.8
0.6
0.4
0.2
0.0
N-terminal (Exon 1-3)
Deleted region (Exon 4-6)
C-terminal (Exon 12)
Hira f/f
Hira f/f, Gdf9-Cre
Hira f/f, Zp3-Cre
D
Ubinuclein 1
Hira
Cabin 1
Hira f/f
Hira f/f, Gdf9-Cre
Cabin 1
Hira
DNA
E
Ubinuclein 1
Hira
Cabin 1
Hira f/f
Hira f/f, Gdf9-Cre
Ubinuclein 1
Hira
DNA
F
Triton pre-extracted
Hira f/f
Hira f/f, Gdf9-Cre
Ubinuclein 1
Hira
DNA
G
Schematic illustration of H3.3B-EGFP knock-in targeting
Wild type allele
5' upstream sequence
Exon1
Exon2
Exon3
Exon4
Exon5
Exon6
3' downstream sequence
H3.3B CDS
Targeting construct
EGFP
IRES
NEO
3' downstream sequence 3.3 kb
PreS
Gb3 Promoter
Targeted allele
5' upstream sequence
Genotyping Primers (1)
Genotyping Primers (2)
3' downstream sequence
PreS EGFP IRES Gb3 Promoter NEO
5.77 kb product amplified by indicated Long Range PCR primers
H3.3B-EGFP ESCs
EC4
DF3
FA5
WT_E14
H3.3B-EGFP mice; F3
1
2
WT mice
1
2
M
10 kb
8 kb
6 kb
5 kb
4 kb
3 kb
2 kb
1.5 kb
1 kb
0.5 kb
Long range PCR; predicted 5.77 kb
H3.3B-EGFP mice; F1
1 2 3 4 5 6 7 8 9 10
ES_FA5
WT mice
1 2
M
500bp
400bp
300bp
200bp
Genotyping primer set 1: predicted product size 260bp
Genotyping primer set 2: predicted product size 272bp

**Figure S1. Oocyte specific depletion of Hira, related to Figure 1.**

(A) Schematic illustration of Hira locus targeting. (B) PCR genotyping confirming genetic recombination in *Hira*$^{f/f}$, *Gdf9-Cre*$^{+}$ GV stage oocytes. (C) qPCR detection of *Hira* mRNA expression levels in zygotes from *Hira*$^{f/f}$, *Hira*$^{f/f}$ *Gdf9-Cre*$^{+}$ or *Hira*$^{f/f}$ *Zp3-Cre*$^{+}$ (oocytes fertilized by wild type sperm). The expression was normalized to exogenous RNA standard and set as 1 in *Hira*$^{f/f}$ zygotes. Error bars indicate s.e.m of three independent experiments. (D-F) CABIN1 (D) or UBN1 (E, F) staining in GV stage oocytes from *Hira*$^{f/f}$ or *Hira*$^{f/f}$ *Gdf9-Cre*$^{+}$ females. Note that CABIN1 was mostly depleted in Hira mutant oocytes (D) and residual amount of UBN1 (E) disappeared after Triton pre-extraction suggesting lack of chromatin association in the absence of Hira (F). DNA was stained with DAPI and shown in blue. Scale bar=10 μm. (G) Schematic illustration of H3.3B-EGFP knock-in targeting and the genotyping results.

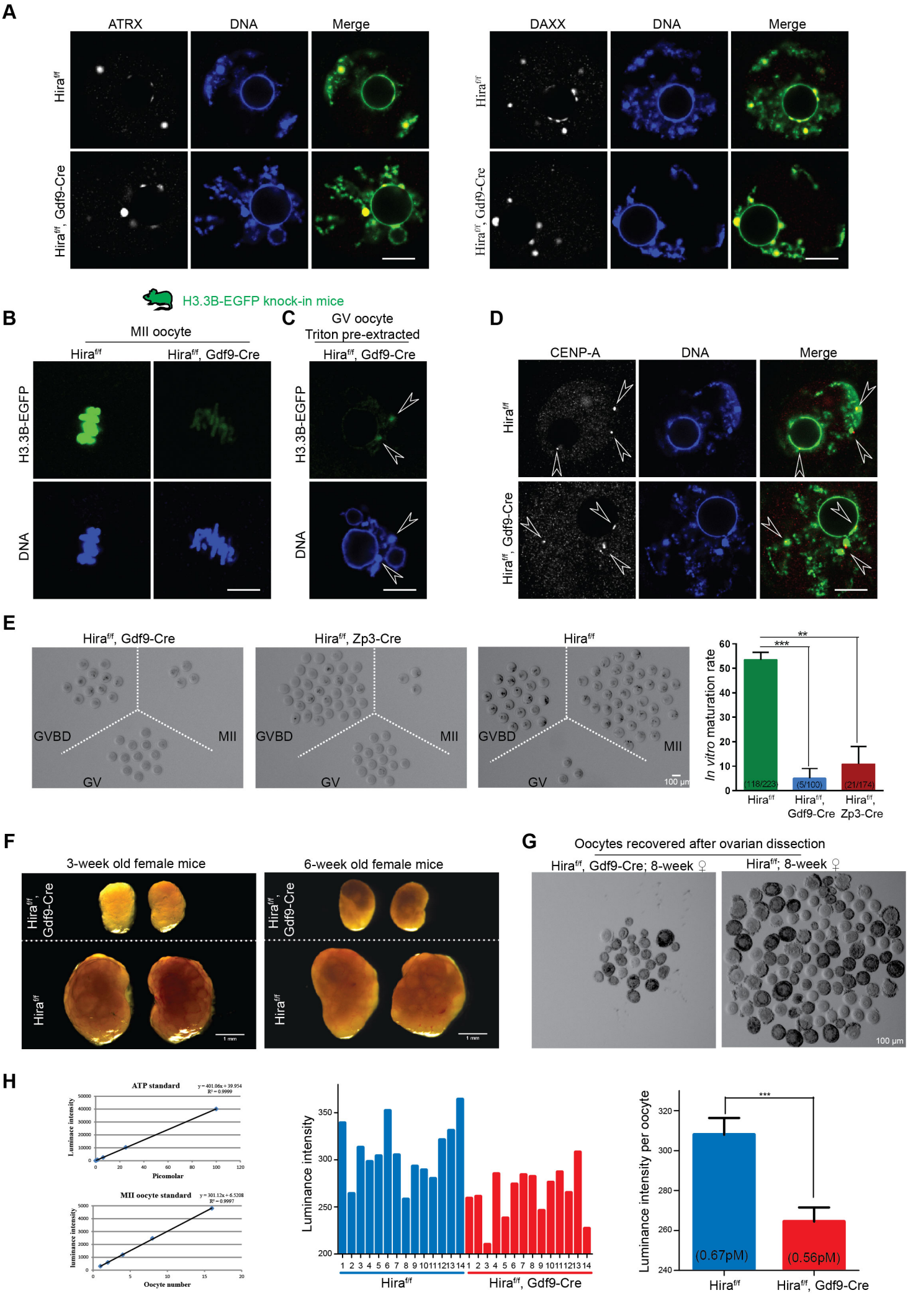
A
ATRX
DNA
Merge
DAXX
DNA
Merge
Hira f/f
Hira f/f, Gdf9-Cre
H3.3B-EGFP knock-in mice
B
MII oocyte
Hira f/f
Hira f/f, Gdf9-Cre
H3.3B-EGFP
DNA
C
GV oocyte
Triton pre-extracted
Hira f/f, Gdf9-Cre
H3.3B-EGFP
DNA
D
CENP-A
DNA
Merge
Hira f/f
Hira f/f, Gdf9-Cre
E
Hira f/f, Gdf9-Cre
Hira f/f, Zp3-Cre
Hira f/f
GVBD
MII
GV
100 μm
In vitro maturation rate
(118/223)
(5/100)
(21/174)
Hira f/f
Hira f/f, Gdf9-Cre
Hira f/f, Zp3-Cre
F
3-week old female mice
6-week old female mice
Hira f/f, Gdf9-Cre
Hira f/f
1 mm
G
Oocytes recovered after ovarian dissection
Hira f/f, Gdf9-Cre; 8-week ♀
Hira f/f; 8-week ♀
100 μm
H
ATP standard
Luminance intensity
Picomolar
MII oocyte standard
Oocyte number
Luminance intensity
Hira f/f
Hira f/f, Gdf9-Cre
Luminance intensity per oocyte
(0.67pM)
(0.56pM)
Hira f/f
Hira f/f, Gdf9-Cre

**Figure S2. Effects of Hira deletion on oocyte development, histone incorporation and on ATRX/DAXX, an alternative H3.3 chaperone complex, related to Figure 1 and Figure 2.**

(A) Maternal Hira depletion did not affect ATRX/DAXX localisation in GV oocytes. (B) Residual H3.3B-EGFP signal could be detected in the MII chromosome in oocytes obtained from *Hira*$^{f/f}$ *Gdf9-Cre*$^{+}$, H3.3B-EGFP mice , the signal is greatly reduced compared to the control. (C) Residual foci of chromatin associated H3.3 (indicated by arrowheads) were detected in Triton pre-extracted *Hira*$^{f/f}$ *Gdf9-Cre*$^{+}$, H3.3B-EGFP GV oocytes following laser intensity enhancement. (D) CENP-A distribution (indicated by arrowheads) was not affected by maternal Hira depletion. DNA was stained with DAPI and shown in blue. Scale bar=10 μm (E) Meiotic competence is greatly reduced in Hira depleted oocytes. GV oocytes were recovered from 3 week old *Hira*$^{f/f}$, *Hira*$^{f/f}$ *Gdf9-Cre*$^{+}$ or *Hira*$^{f/f}$ *Zp3-Cre*$^{+}$ females and cultured for 16 hours. Meiotic maturation was judged by the first polar body extrusion. Representative bright field images of the oocytes after overnight incubation are shown on the left; quantification graph is shown on the right. (F) Representative images of three independent experiments showing ovaries of *Hira*$^{f/f}$ or *Hira*$^{f/f}$ *Gdf9-Cre*$^{+}$ siblings at 3 or 6 weeks of age. Images were taken in a single picture. (G) Representative images of oocytes recovered after ovarian dissection of 8 week old *Hira*$^{f/f}$ or *Hira*$^{f/f}$ *Gdf9-Cre*$^{+}$ siblings. Dissections were carried out twice at 8 week and twice at 5 week old stages (data not shown). Scale bars as indicated. (H) Quantification of ATP levels in single MII oocytes. Standard curve for ATP of oocytes is shown on the left. Luminance intensity of single MII oocyte ATP level (middle). 14 MII oocytes collected from two *Hira*$^{f/f}$ or two *Hira*$^{f/f}$ *Gdf9-Cre*$^{+}$ females were subjected to ATP measurement. Quantification of average level of ATP content in single MII oocytes (right). Absolute ATP content was calculated using the standard curves and indicated in each column. In all cases, error bars indicate s.e.m.; ns, non-significant; *, $p<0.05$; **, $p<0.01$; ***, $p<0.001$.

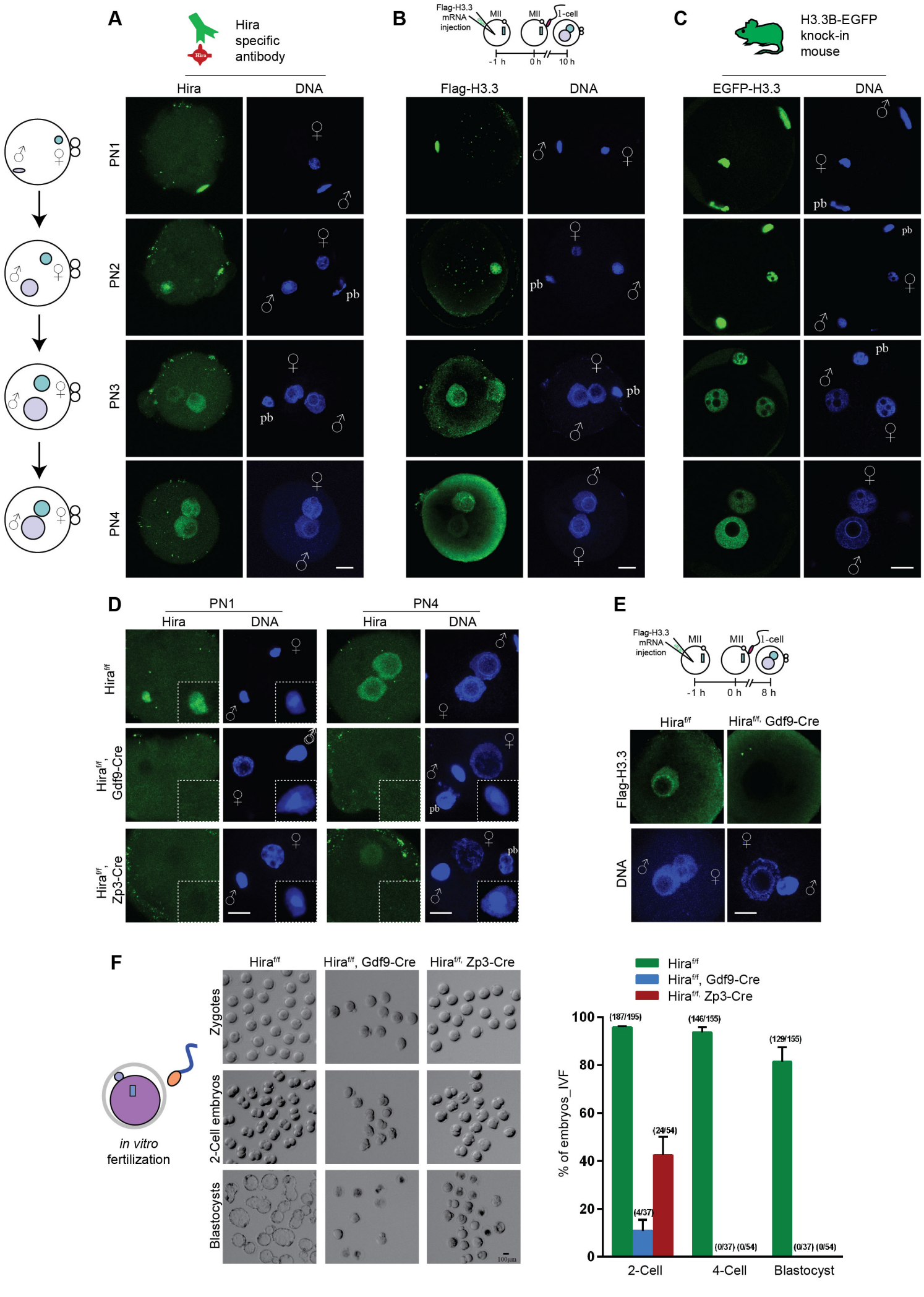
A
Hira specific antibody
Hira
DNA
PN1
PN2
PN3
PN4
pb
B
Flag-H3.3 mRNA injection
MII
MII
1-cell
-1 h
0 h
10 h
Flag-H3.3
DNA
C
H3.3B-EGFP knock-in mouse
EGFP-H3.3
DNA
D
PN1
PN4
Hira
DNA
Hira f/f
Hira f/f, Gdf9-Cre
Hira f/f, Zp3-Cre
E
Flag-H3.3 mRNA injection
MII
MII
1-cell
-1 h
0 h
8 h
Hira f/f
Hira f/f, Gdf9-Cre
Flag-H3.3
DNA
F
Hira f/f
Hira f/f, Gdf9-Cre
Hira f/f, Zp3-Cre
Zygotes
2-Cell embryos
Blastocysts
100μm
in vitro fertilization
% of embryos_IVF
100
80
60
40
20
0
(187/195)
(4/37)
(24/54)
(146/155)
(0/37)
(0/54)
(129/155)
(0/37)
(0/54)
2-Cell
4-Cell
Blastocyst

**Figure S3. Maternal Hira is necessary for H3.3 incorporation in zygotes, related to Figure 2.**

(A) Localisation of Hira during mouse zygotic development. (B) H3.3 incorporation in mouse zygotes following microinjection of Flag-H3.3 mRNA. Zygotes were fixed at different PN stages and stained with anti-Flag antibody. (C) H3.3B-EGFP distribution in mouse zygotes. MII oocytes were collected from 3-week old *H3.3B-EGFP* knock-in females and fertilised *in vitro* by wild type sperm. Zygotes were fixed at different PN stages and stained with anti-GFP antibody. (D) Hira protein is completely absent from zygotes obtained by *in vitro* fertilisation of *Hira*$^{f/f}$ *Gdf9-Cre*$^{+}$ or *Hira*$^{f/f}$ *Zp3-Cre*$^{+}$ MII oocytes with wild type sperm. An enlarged image of paternal pronucleus is shown in the insets. Note that paternal genome underwent only partial de-condensation. (E) Maternal Hira is necessary for H3.3 incorporation into the paternal pronucleus. *Hira*$^{f/f}$ or *Hira*$^{f/f}$ *Gdf9-Cre*$^{+}$ MII oocytes were microinjected with Flag-H3.3 mRNA and *in vitro* fertilised by wild type sperm. Zygotes were fixed and stained by anti-Flag antibody 8 hours later. (F) Early developmental arrest of embryos with maternal Hira depletion. MII oocytes were collected from *Hira*$^{f/f}$, *Hira*$^{f/f}$ *Gdf9-Cre*$^{+}$ or *Hira*$^{f/f}$ *Zp3-Cre*$^{+}$ females following hormonal stimulation and fertilised *in vitro* by wild type sperm prior to *in vitro* culture. Representative images of embryos (left panel); quantification of developmental progression (right panel). Embryo numbers are indicated above each column. Zygotes depleted of Hira do not progress beyond the two-cell stage. DNA is stained by DAPI (blue). ♀, female pronucleus; ♂, male pronucleus; pb, polar body. Scale bar= 10μm

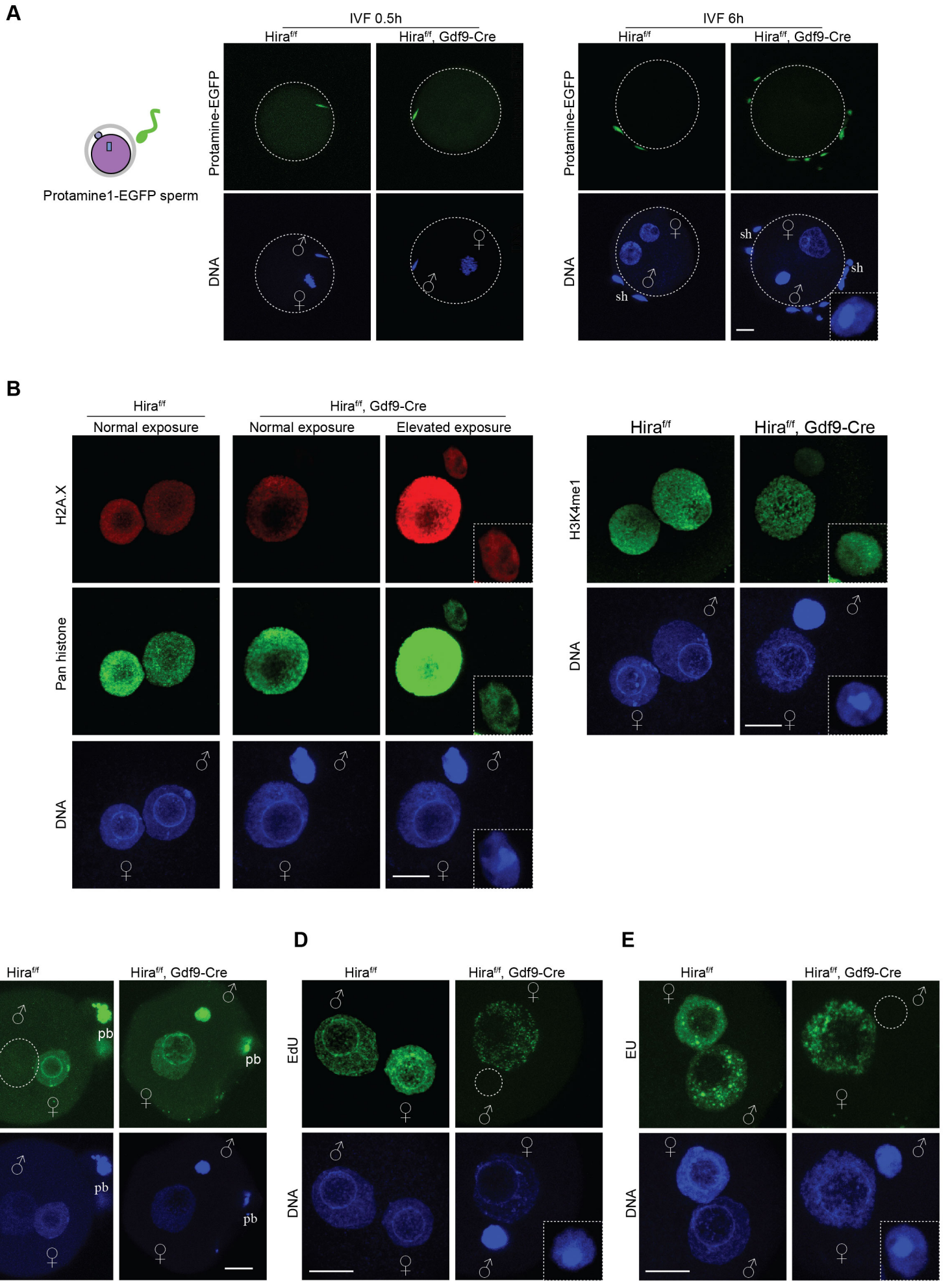
A
IVF 0.5h
IVF 6h
Hira f/f
Hira f/f, Gdf9-Cre
Protamine-EGFP
DNA
Protamine1-EGFP sperm
sh
B
Hira f/f
Hira f/f, Gdf9-Cre
Normal exposure
Elevated exposure
H2A.X
Pan histone
H3K4me1
C
5mC
pb
D
EdU
E
EU

**Figure S4. Maternal Hira depleted oocytes fail to reprogramme paternal genome after fertilisation, related to Figure 2.**

(A) Protamine removal is not affected by maternal Hira depletion. MII ooyctes collected from *Hira*$^{f/f}$ *Gdf9-Cre*$^{+}$ females were fertilized *in vitro* by sperm collected from *protamine1-EGFP* transgenic adult male mice. Zygotes were fixed at the indicated time points. Note that protamines were detectable in the paternal genome 0.5h after insemination but were not detectable afterwards. Sperm heads, which could not enter the oocyte, were used as positive control for Protamine 1 staining. Oocytes from *Hira* $^{f/f}$ siblings were used as control. (B) Paternal pronucleus of zygotes maternally depleted for Hira contains residual histones. *Hira*$^{f/f}$ or *Hira*$^{f/f}$ *Gdf9-Cre*$^{+}$ oocytes were fertilised *in vitro* by wild type sperm. The zygotes were fixed 10 hours later and simultaneously stained with anti-H2A.X, anti-pan histone antibodies (left) or for the presence of H3K4me1 (right). (C) DNA demethylation did not occur in the partially decondensed paternal genome of Hira mutant zygote. MII oocytes obtained from *Hira*$^{f/f}$ or *Hira*$^{f/f}$ *Gdf9-Cre*$^{+}$ females were fertilised *in vitro* by wild type sperm. The zygotes were fixed at PN4-5 stages and stained with anti-5mC antibody. DNA was stained by PI and pseudocoloured in blue. (D, E) Representative images for detection of DNA replication by EdU labelling (D) or of nascent RNA synthesis by EU labelling (E). MII oocytes collected from *Hira*$^{f/f}$ or *Hira*$^{f/f}$ *Gdf9-Cre*$^{+}$ siblings were fertilized *in vitro* by wild type sperm and cultured in presence of EdU (D) or EU (E) and fixed at PN4-5 stage. Note that neither replication nor transcription was detected in the partially decondensed paternal pronucleus in maternal Hira deleted zygotes. Enlarged image of paternal pronucleus is shown in the inset (b,d,e). ♀, female pronucleus; ♂, male pronucleus; pb, polar body. sh, sperm head. Scale bar= 10 μm

A

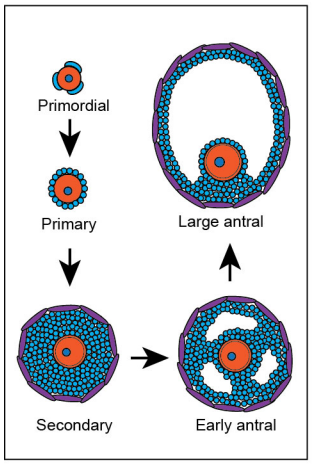
Primordial
Primary
Large antral
Secondary
Early antral

C

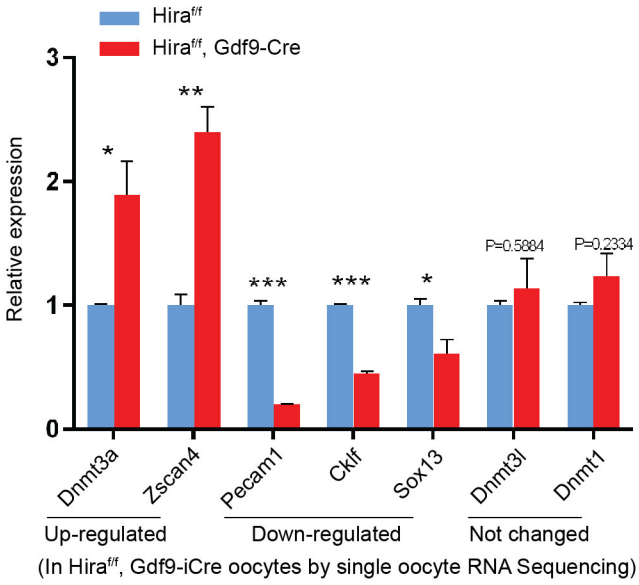
Hira$^{f/f}$
Hira$^{f/f}$, Gdf9-Cre
Relative expression
3
2
1
0
*
**
***
***
*
P=0.5884
P=0.2334
Dnmt3a
Zscan4
Pecam1
Cklf
Sox13
Dnmt3l
Dnmt1
Up-regulated
Down-regulated
Not changed
(In Hira$^{f/f}$, Gdf9-iCre oocytes by single oocyte RNA Sequencing)

B

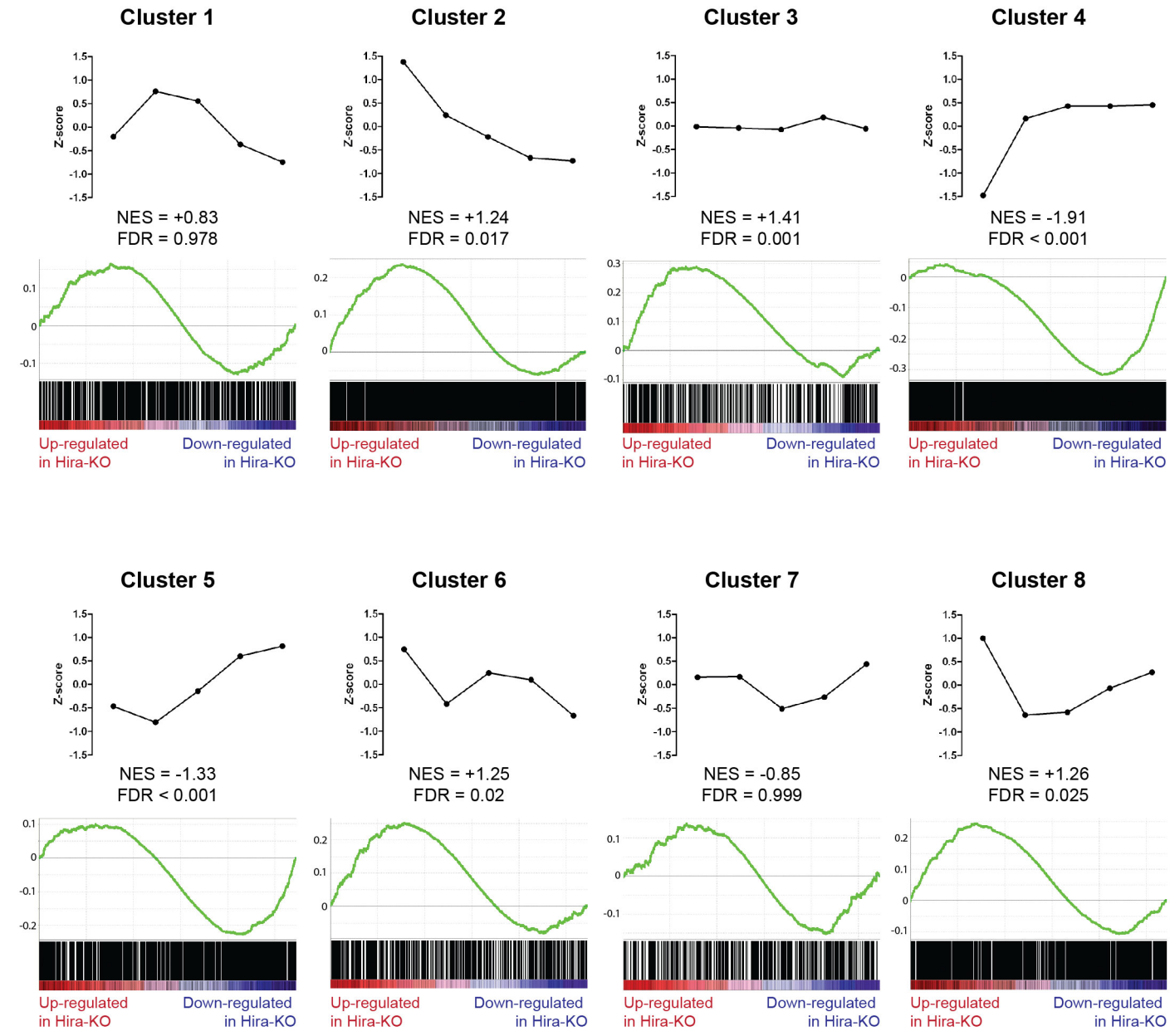
Cluster 1
NES = +0.83
FDR = 0.978
Cluster 2
NES = +1.24
FDR = 0.017
Cluster 3
NES = +1.41
FDR = 0.001
Cluster 4
NES = -1.91
FDR < 0.001
Cluster 5
NES = -1.33
FDR < 0.001
Cluster 6
NES = +1.25
FDR = 0.02
Cluster 7
NES = -0.85
FDR = 0.999
Cluster 8
NES = +1.26
FDR = 0.025
Z-score
Up-regulated in Hira-KO
Down-regulated in Hira-KO

**Figure S5. Relationship between gene expression changes in Hira depleted oocytes and transcriptional dynamics during oogenesis, related to Figure 5.**

(A) Schematic illustration of developmental stages during oogenesis. Adapted from previous publications (Li and Albertini, 2013; Pan et al., 2005). (B) Gene set enrichment analysis (GSEA) comparing gene expression patterns during oogenesis (Pan et al., 2005) and the ranked list of gene expression changes in *Hira*$^{f/f}$ *Gdf9-Cre*$^{+}$ relative to *Hira*$^{f/f}$ MII oocytes. NES - Normalised Enrichment Score; FDR – False Discovery Rate (calculated in GSEA program). For each cluster, each dot represents mean-normalised gene expression for consecutive stages of oocyte development. (C) qPCR validation of Hira$^{f/f}$, GDF9-Cre$^{+}$ single oocyte RNA sequencing. A range of genes were selected from RNA sequencing data and the expression was normalized to exogenous RNA standard and set as 1 in *Hira*$^{f/f}$ zygotes. Error bars indicate s.e.m of three technical replicates.

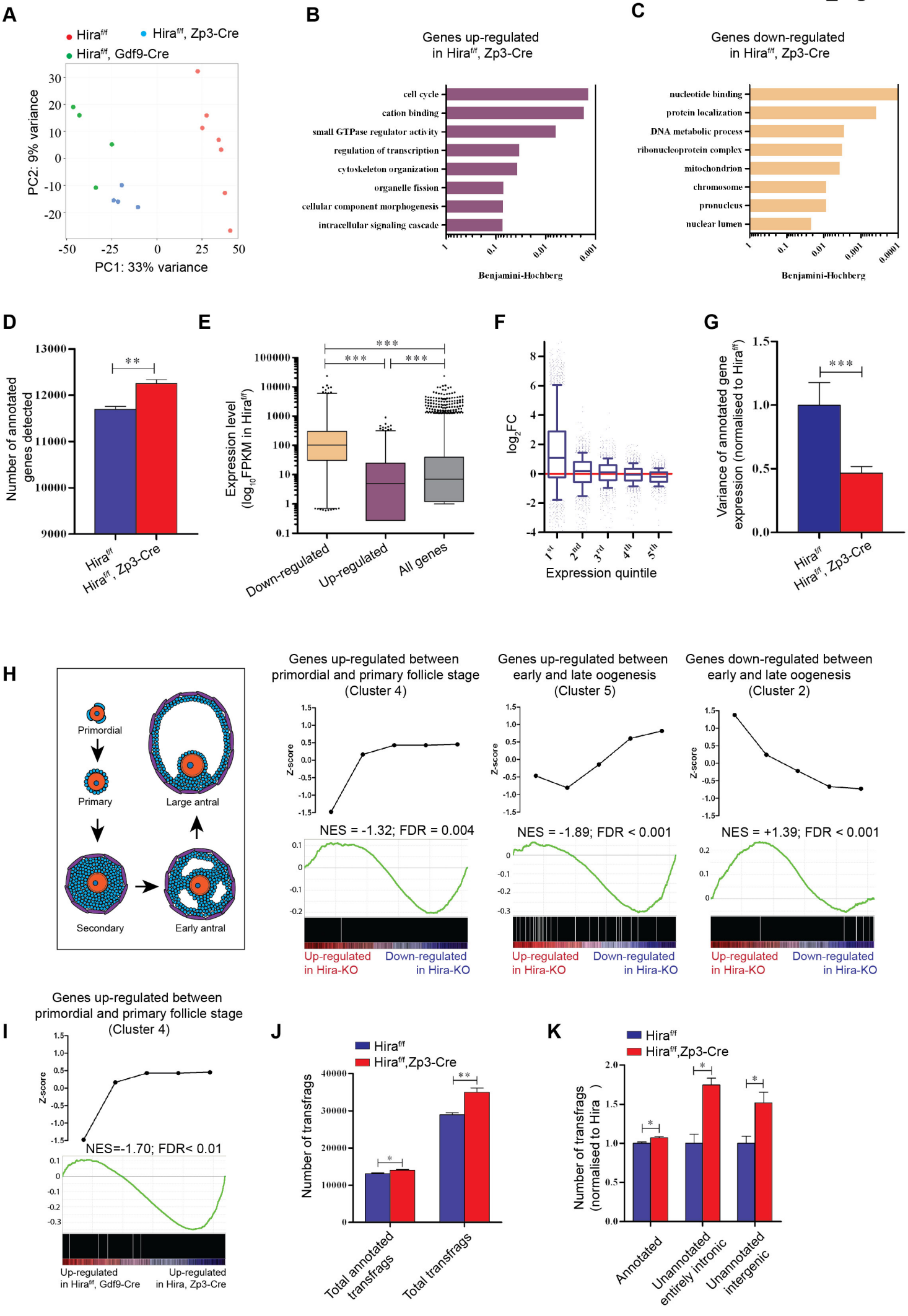
A
Hira f/f
Hira f/f, Zp3-Cre
Hira f/f, Gdf9-Cre
PC2: 9% variance
PC1: 33% variance
B
Genes up-regulated in Hira f/f, Zp3-Cre
cell cycle
cation binding
small GTPase regulator activity
regulation of transcription
cytoskeleton organization
organelle fission
cellular component morphogenesis
intracellular signaling cascade
Benjamini-Hochberg
C
Genes down-regulated in Hira f/f, Zp3-Cre
nucleotide binding
protein localization
DNA metabolic process
ribonucleoprotein complex
mitochondrion
chromosome
pronucleus
nuclear lumen
Benjamini-Hochberg
D
Number of annotated genes detected
Hira f/f
Hira f/f, Zp3-Cre
E
Expression level (log10FPKM in Hira f/f)
Down-regulated
Up-regulated
All genes
F
log2FC
Expression quintile
G
Variance of annotated gene expression (normalised to Hira f/f)
Hira f/f
Hira f/f, Zp3-Cre
H
Primordial
Primary
Large antral
Secondary
Early antral
Genes up-regulated between primordial and primary follicle stage (Cluster 4)
Z-score
NES = -1.32; FDR = 0.004
Up-regulated in Hira-KO
Down-regulated in Hira-KO
Genes up-regulated between early and late oogenesis (Cluster 5)
NES = -1.89; FDR < 0.001
Genes down-regulated between early and late oogenesis (Cluster 2)
NES = +1.39; FDR < 0.001
I
Genes up-regulated between primordial and primary follicle stage (Cluster 4)
NES=-1.70; FDR< 0.01
Up-regulated in Hira f/f, Gdf9-Cre
Up-regulated in Hira, Zp3-Cre
J
Hira f/f
Hira f/f,Zp3-Cre
Number of transfrags
Total annotated transfrags
Total transfrags
K
Hira f/f
Hira f/f,Zp3-Cre
Number of transfrags (normalised to Hira )
Annotated
Unannotated entirely intronic
Unannotated intergenic

**Figure S6. Hira$^{f/f}$, Zp3-Cre$^{+}$ Single Oocyte RNA sequencing, related to Figure 4 and Figure 5.**

(A) PCA plot of scRNA-Seq data derived from *Hira*$^{f/f}$, *Hira*$^{f/f}$ *Gdf9-Cre*$^{+}$, and *Hira*$^{f/f}$ *Zp3-Cre*$^{+}$ MII oocytes; PC1 and PC2 refer to the first and second principle components, respectively. Hira-wild type and Hira-knockout oocytes are clearly distinguishable by PC1 (note: Hira$^{f/f}$ samples were used to correct for batch effect). (B, C) Selected gene ontology (GO) terms significantly enriched for among differentially up-regulated (B, EdgeR, FDR < 0.1) and differentially down-regulated (C, EdgeR, FDR < 0.1) genes in *Hira*$^{f/f}$ *Zp3-Cre*$^{+}$ MII oocytes. X-axis represents the Benjamini-Hochberg adjusted p value. (D) Number of annotated genes detected, as computed by HTSeq programme. (E) Boxplot of gene expression levels of differentially up- or down-regulated genes between *Hira*$^{f/f}$ *Zp3-Cre*$^{+}$ and *Hira*$^{f/f}$ MII oocytes (EdgeR, FDR < 0.1), and all annotated genes. (F) Box plots showing distribution of gene expression fold-change for each gene expression level quintile (based on *Hira*$^{f/f}$ gene-expression levels). (G) Variance of gene expression within a given *Hira*$^{f/f}$ or *Hira*$^{f/f}$ *Zp3-Cre*$^{+}$ sample. (H) Gene set enrichment analysis (GSEA) comparing genes of selected expression clusters during oogenesis (Figure S6) and the ranked list of gene expression changes in *Hira*$^{f/f}$ *Zp3-Cre*$^{+}$ MII oocytes relative to *Hira*$^{f/f}$ oocytes. NES - Normalised Enrichment Score; FDR - False Discovery Rate (both calculated in GSEA program). For each cluster, each dot represents mean-normalised gene expression for consecutive stages of oocyte development. (I) GSEA comparing genes of cluster 4 (i.e. specifically up-regulated between primordial and primary stages) and the ranked list of gene expression changes in *Hira*$^{f/f}$ *Gdf9-Cre*$^{+}$ MII oocytes relative to and *Hira*$^{f/f}$ *Zp3-Cre*$^{+}$ MII oocytes. NES - Normalised Enrichment Score; FDR - False Discovery Rate (both calculated in GSEA program). (J) Number of total transfrags and total annotated transfrags in *Hira*$^{f/f}$ and *Hira*$^{f/f}$ *Zp3-Cre*$^{+}$ MII oocytes (as computed by CuffCompare program). (K) Number of total annotated transfrags, unannotated

entirely intronic transfrags, and unannotated entirely intergenic transfrags in *Hira*$^{f/f}$ and *Hira*$^{f/f}$ *Zp3-Cre*$^{+}$ MII oocytes (as computed by CuffCompare program). In all cases error bars indicate s.e.m.; ns, non-significant; *, $p<0.05$; **, $p<0.01$; ***, $p<0.001$. Statistical analysis was carried out using two-tailed unpaired Student's t-test (D, I, J), Kruskal-Wallis with Dunn's post-hoc test (E) or F-test (G).

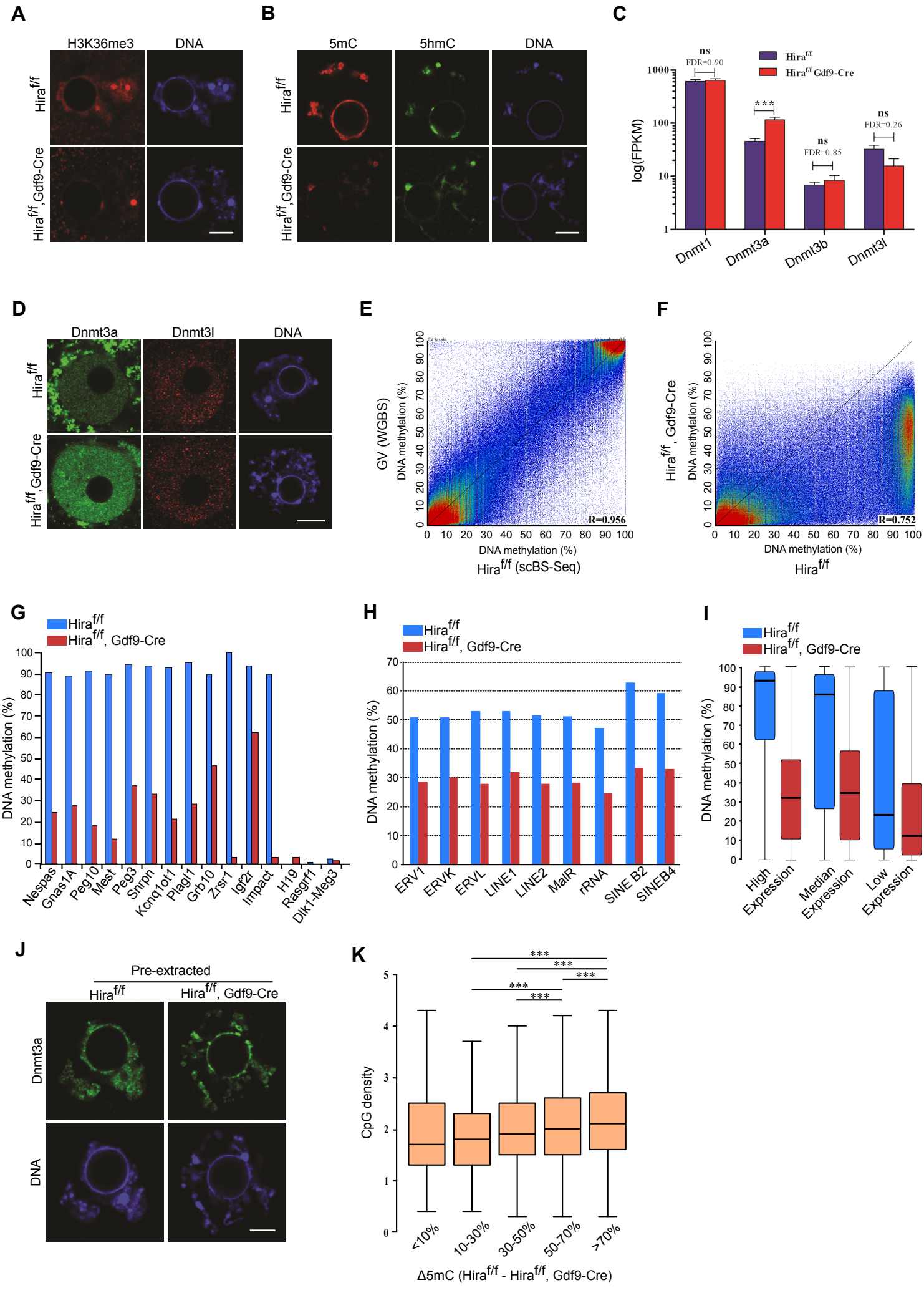
A
H3K36me3
DNA
Hira f/f
Hira f/f,Gdf9-Cre
B
5mC
5hmC
DNA
C
ns
FDR=0.90
***
ns
FDR=0.85
ns
FDR=0.26
Hira f/f
Hira f/f Gdf9-Cre
log(FPKM)
Dnmt1
Dnmt3a
Dnmt3b
Dnmt3l
D
Dnmt3a
Dnmt3l
DNA
E
GV (WGBS)
DNA methylation (%)
R=0.956
Hira f/f (scBS-Seq)
F
Hira f/f, Gdf9-Cre
R=0.752
G
Hira f/f
Hira f/f, Gdf9-Cre
DNA methylation (%)
Nespas
Gnas1A
Peg10
Mest
Peg3
Snrpn
Kcnq1ot1
Plagl1
Grb10
Zrsr1
Igf2r
Impact
H19
Rasgrf1
Dlk1-Meg3
H
ERV1
ERVK
ERVL
LINE1
LINE2
MalR
rRNA
SINE B2
SINEB4
I
High Expression
Median Expression
Low Expression
J
Pre-extracted
Dnmt3a
DNA
K
CpG density
<10%
10-30%
30-50%
50-70%
>70%
Δ5mC (Hira f/f - Hira f/f, Gdf9-Cre)

**Figure S7. Further characterisation of global DNA hypomethylation observed in Hira depleted oocytes, related to Figure 6.**

(A) Global H3K36me3 levels are lower in *Hira*$^{f/f}$, *Gdf9-Cre*$^{+}$ oocytes as judged by immunofluorescence staining. (B) Immunofluorescence staining showing the reduction of global 5-methylcytosine (5mC) and comparable level of 5-hydroxymethylcytosine (5hmC) in *Hira*$^{f/f}$ and *Hira*$^{f/f}$, *Gdf9-Cre*$^{+}$ GV oocyte. (C) Expression levels of DNA methyltransferases in *Hira*$^{f/f}$ and *Hira*$^{f/f}$, *Gdf9-Cre*$^{+}$; False Discovery Rate (FDR) was computed by the edgeR programme. (D) Immunofluorescence staining of Dnmt3a and Dnmt3l. Note the elevated levels of Dnmt3a and comparable level of Dnmt3l in *Hira*$^{f/f}$, *Gdf9-Cre*$^{+}$ GV oocytes. (E, F) Scatter plot visualisation of DNA methylation (3-kb sliding windows, 1.5kb steps) for published GV WGBS data (Shirane et al., 2013) versus *Hira*$^{f/f}$ oocytes (E), and *Hira*$^{f/f}$ versus *Hira*$^{f/f}$, *Gdf9-Cre*$^{+}$ *oocyte* (F); Correlation value (R) is based on Pearson's test. (G) Quantification of DNA methylation at imprinted germline DMRs in *Hira*$^{f/f}$, and *Hira*$^{f/f}$, *Gdf9-Cre*$^{+}$ oocytes. (H) Quantification of DNA methylation at various repeat families in *Hira*$^{f/f}$, and *Hira*$^{f/f}$, *Gdf9-Cre*$^{+}$ oocytes. (I) Effects on DNA methylation in Hira deleted oocytes are more pronounced at highly expressed genes. DNA methylation was quantified for genes defined as high, median, low expressed based on our RNA-Seq data for each genotype. (J) Immunofluorescence staining of Triton pre-extracted GV oocytes. Note that Dnmt3a is chromatin associated in both *Hira*$^{f/f}$ and *Hira*$^{f/f}$, *Gdf9-Cre*$^{+}$ GV oocytes. (K) 3kb probes normally methylated in control oocytes (>80% methylation in *Hira*$^{f/f}$ oocytes) were binned according to their difference in DNA methylation between *Hira*$^{f/f}$ and *Hira*$^{f/f}$, *Gdf9-Cre*$^{+}$, CpG density of the probes was calculated and reported as a boxplot (***: $p<0.001$, Kruskall-Wallis test).

**Supplemental Table Legends**

**Table S1. Summary of differential gene expression analysis between *Hira*$^{f/f}$ *Gdf9-Cre*$^{+}$ and *Hira*$^{f/f}$ MII oocytes, related to Figure 4.**

The log fold change (LogFC), p-value (PValue), and false discovery rate (FDR) were computed by EdgeR software; the FPKM values for each gene for each sample were computed using HTSeq and custom R script.

**Table S2. Summary of *de novo* transcript assembly using CuffCompare for *Hira*$^{f/f}$ *Gdf9-Cre*$^{+}$ and *Hira*$^{f/f}$ MII oocytes, related to Figure 5.**

The transcript ID, transcript class, and FPKM for each transcript for each sample were computed using CuffCompare software.

**Table S3. Summary of differential gene expression analysis between *Hira*$^{f/f}$ *Zp3-Cre*$^{+}$ and *Hira*$^{f/f}$ MII oocytes, related to Figure 4 and Figure S8.**

The log fold change (LogFC), p-value (PValue), and false discovery rate (FDR) were computed by EdgeR software; the FPKM values for each gene for each sample were computed using HTSeq and custom R script.

**Table S4. Summary of *de novo* transcript assembly using CuffCompare for *Hira*$^{f/f}$ *Zp3-Cre*$^{+}$ and *Hira*$^{f/f}$ MII oocytes, related to Figure 5 and Figure S8.**

The transcript ID, transcript class, and FPKM for each transcript for each sample were computed using CuffCompare software.

## Supplemental Experimental Procedures

### Mice

Hira (*Hira*$^{f/f}$) mice were generated by the Wellcome Trust Sanger Institute (UK). Oocyte-specific Hira depletion was achieved by crossing *Hira*$^{f/f}$ mice with *Gdf9-iCre* (Lan et al., 2004) or with *Zp3-Cre* mice (de Vries et al., 2000) (obtained from Prof A. Surani, Cambridge, UK), respectively.

The *H3.3B-EGFP* knock-in mouse was generated in the MRC transgenic facility by standard protocol. The knock-in vector was provided by Prof R. Festenstein and transfected into E14 ES cells by electroporation. Positive ES clones were injected into C57B6-derived E3.5 blastocysts and implanted into 2.5 days post-coitum pseudo-pregnant female mice. Germline transmission was assessed by chimaerism in the pups.

Protamine 1-EGFP mice (Haueter et al., 2010) were re-derived and provided by Dr. P. Pelczar. All mutant mice strains were of C57B6 genetic background. All animal experiments were carried out under a UK Home Office Project Licence in a Home-Office designated facility.

### *In vitro* fertilisation (IVF), *in vitro* maturation (IVM) and parthenogenesis

IVF and parthenogenesis were carried out as described previously (Nashun et al., 2010). Briefly, three weeks old mice were super-ovulated by intraperitoneal injection using 5 IU pregnant mare's serum gonadotropin (PMSG) and 5 IU of human chorionic gonadotropin (hCG) 48 hours later. For *in vitro* fertilization, the cumulus-oocyte complexes were transferred to HTF medium supplemented with 10 mg/ml BSA (Sigma-Aldrich) and inseminated with capacitated spermatozoa obtained from the caudal epididymides of adult B6CBAF1 male mice (Charles River or Harlan, UK). The spermatozoa capacitation was

achieved by pre-incubating for 2 h in HTF medium. Fertilized oocytes were washed in HTF and cultured in KSOM. Oocyte numbers were counted after digesting the cumulus-oocyte complexes with 0.3mg/ml hyaluronidase (Sigma-Aldrich), or four hours after insemination in the case of IVF.

Germinal vesicle (GV) stage oocytes were obtained from 3-week old females as described previously (Nashun et al., 2010). The ovaries were removed and transferred to M2 medium supplemented with 0.2 mM 3-isobutyl-1-methylxanthine (IBMX; Sigma-Aldrich). The ovarian follicles were punctured with a 26-gauge needle, and a narrow-pore glass pipette was used to remove the cumulus cells from the cumulus-oocyte complexes. For *in vitro* maturation, GV-oocytes were then transferred to α-minimal essential medium (Life Technologies,) containing 5% fetal bovine serum (FBS; Sigma-Aldrich), and 10 ng/ml epidermal growth factor (EGF; Sigma-Aldrich). Oocyte maturation was assessed by the first polar body extrusion after 16 hours incubation. Similarly, growing oocytes were collected from ovaries of 14 to 16 days old mice in M2 medium.

**Immunofluorescence staining of mouse oocytes and zygotes**

Oocytes and embryos were fixed for 20 minutes in PBS containing 4% paraformaldehyde (PFA) at room temperature and washed with 1% BSA/PBS three times unless otherwise stated. The cells were permeabilized by incubating in 1% BSA/PBS containing 0.5% Triton X-100 for 30 min at room temperature, and, after washing with 1% BSA/PBS three times, incubated with primary antibodies in 1% BSA/PBS containing 0.1% Triton X-100 overnight at 4ºC, washed three times, and incubated for 1 hour in the dark with Alexa Fluor 488- and/or 568-conjugated IgG secondary antibody (dilution 1:300, Molecular probes) in the same buffer. DNA was stained for 10 minutes with 3 μg/ml 4,6-diamidimo-2-phenylindole (DAPI) and the cells were then mounted either with Vectashield solution (Vector Laboratories) on

glass slides for single section imaging or with ProLong Gold mounting medium (Life Technologies) for sequential Z-stack imaging. Fluorescence was detected using a Leica TCS SP5 confocal microscope with a 63x objective and Z-step size of 0.5 μm in the case of Z-stack scanning. More than 12 oocytes/zygotes were examined in each immunofluorescence staining panel unless otherwise specified.

**Primary antibody list:**

| Antibody target | Host | Supplier/Catalogue number | Dilution |
|---|---|---|---|
| Hira | Mouse | Millipore; #04-1488. | 1:100 |
| UBN1 | Rabbit | Sigma-Aldrich; SAB4501346. | 1:100 |
| CABIN1 | Rabbit | Abcam; Ab3349. | 1:100 |
| ATRX | Rabbit | Santa Cruz; SC-15408. | 1:100 |
| DAXX | Rabbit | Santa Cruz; SC-7152. | 1:100 |
| Pan histone | Mouse | Millipore; MAB3422. | 1:100 |
| H2A.X | Rabbit | Abcam; Ab11175. | 1:100 |
| γ-H2A.X | Mouse | Millipore; JBW301. | 1:100 |
| EGFP | Goat | Abcam; Ab5450. | 1:200 |
| Flag-epitope | Mouse | Sigma; F1804. | 1:100 |
| CENP-A | Rabbit | Cell Signalling; 2048. | 1:100 |
| H3K4me1 | Rabbit | Abcam; AB8895. | 1:200 |
| H3K27me3 | Rabbit | Cell Signalling; 9756. | 1:400 |
| H3K36me3 | Rabbit | Abcam; AB9050. | 1:400 |
| Dnmt3a | Mouse | Imgenex; IMG268. | 1:200 |
| Dnmt3l | Mouse | Abnova; PAB2230. | 1:100 |
| EGFP | Goat | Abcam; AB5450. | 1:100 |

**5-methylcytosine (5mC) staining in oocytes and zygotes**

The staining was carried out as described previously (Hajkova et al., 2010). Briefly, zygotes were fixed for 20min with 4% PFA and permeabilized for 40 min with 0.5% Triton X-100 in 1% BSA/PBS, treated with 10 mg/ml RNase A (Roche) in 1% BSA/PBS for 1 hour at 37$^{o}$C, and incubated in 4N HCl for 15 min at 37$^{o}$C to denature genomic DNA, followed by a 10 min wash in 1% BSA/PBS. After incubating for 30 min at room temperature in 1% BSA/PBS containing 0.1% Triton X-100, the cells were incubated with anti-5mC antibody (Diagenode, clone 33D3, 1:5000 dilution) at 4$^{o}$C overnight in the same buffer. Zygotes were subsequently

washed three times in 1% BSA/PBS containing 0.1% Triton X-100 for 10 min and incubated with Alexa Fluor 405-conjugated IgG secondary antibodies (dilution 1:300, Molecular Probes) for 1 hour in dark at room temperature. DNA was stained with propidium iodide (PI) (0.25mg/ml). After the final wash in 1% BSA/PBS for 30 min, the oocytes or zygotes were mounted in ProLong Gold mounting medium without DAPI (Life Technologies).

**RNA preparation and RT-PCR analysis**

Total RNA was purified using Trizol (Life Technologies). RNA from 20 zygotes was collected in 1ml Trizol in the presence of 10 pg of an exogenous RNA standard. Reverse transcription was performed using PrimeScript RT Reagent Kit with gDNA Eraser (Takara Bio, RR047A). cDNA corresponding to 2 zygotes was analysed using SensiMix SYBR No-ROX (Bioline) in a CFX96 real-time PCR detection system (Bio-Rad). Relative expression was normalized to exogenous standard and two-tailed unpaired t-test was performed. Primers:

| Primer name | Sequence(5'-3') |
|---|---|
| Hira exon 1-3_F | AAGCTCTTGAAGCCAACCTG |
| Hira exon 1-3_R | GGCAAAGCATCTTGGGAATA |
| Hira exon 4-6_F | TTAGCTTCTGGGGGAGATGA |
| Hira exon 4-6_R | CATCACATCGCCTGAGTGAC |
| Hira exon 12_F | GCCGAATTCACCAGTCTACC |
| Hira exon 12_R | ACTTTCCCCATTGACCACAC |

**Detection of DNA replication and transcription in zygotes and oocytes**

In order to detect DNA replication or general transcription, fertilized oocytes were transferred into medium containing 400uM of 5-ethynyl deoxyuridine (EdU, included in C10337, Life Technologies) 4 hours after insemination or 1mM of 5-ethynyl uridine (EU, included in C10329, Life Technologies) 6 hours after insemination, respectively. Zygotes were collected at 10 hours after insemination and zona pellucida was removed by Tyrode's acidic solution before fixation in PFA 4% for 20 min at room temperature. Growing or GV oocytes were

incubated for 4 hours with 400uM of EdU prior to fixation. EU or EdU staining was done according to manufacturer's instruction.

**TUNEL assay detection of the DNase I sensitivity**

*Hira*$^{f/f}$ or *Hira* mutant GV-oocytes were collected from siblings of the same litter as described above and pre-extracted immediately in ice-cold solution (50 mM NaCl, 3 mM $MgCl_2$, 0.5% Triton X-100, 300 mM sucrose in 25 mM HEPES pH 7.4) for 5 min. The oocytes were then incubated with different concentrations (0.1, 0.01or 0.001 U/μL) of DNase 1 (NEB) for 5 min at 37 $^{o}$C in the same buffer without Triton X-100 and fixed for 10 min in 2% PFA/PBS at room temperature. TUNEL assay was done using Click-iT TUNEL Alexa Fluor Imaging Assay (Life Technologies, C10245) according to manufacturer's instructions.

***In vitro* mRNA synthesis and microinjection**

The cDNA sequence of human histone H3.1 (Dr. T. Bartke, MRC Clinical Sciences Centre) or H3.2, H3.3 (Prof. N.Dillon, MRC Clinical Sciences Centre) was subcloned into pGEM-T Easy Vector (Promega) and Flag-epitope tag was added at N-terminal tail by PCR amplification. Plasmids containing Flag-H2A.X and Flag-H4 were obtained from Prof.F.Aoki (University of Tokyo). *In vitro* mRNA synthesis and microinjections were performed as described previously (Nashun et al., 2010). Briefly, plasmids were linearized by appropriate restriction enzymes (NEB). 5'-capped mRNAs were synthesized using Sp6 or T7 mMessage mMachine kit (Ambion) and poly (A) tails were added by a Poly (A) Tailing Kit (Ambion). Finally, the DNA template was removed by Turbo DNase treatment and synthesized mRNA was extracted by phenol/chloroform extraction followed by isopropanol precipitation. Microinjection was performed under an inverted microscope (Eclipse TE200; Nikon) using a micromanipulator (Narishige) and microinjector (Medical System Pico-Injector PLI-100).

Approximately 10 pl synthetic RNA (~200 μg/ml) was microinjected into the cytoplasm of oocytes or embryos.

**Haematoxylin & Eosin (H&E) staining of ovarian sections**

Ovarian tissues were fixed in 4% paraformaldehyde overnight at 4 $^{o}$C and embedded in O.C.T and stored at -80 $^{o}$C before use. 10 μm sections were prepared using a Leica CM1950 cryomicrotome (Leica Microsystems). For H&E staining, the sections were air dried for several minutes to remove moisture and stained with filtered 0.1% Mayers Hematoxylin (Sigma-Aldrich, MHS-16) for 10 minutes. Then, rinsed in cool running water for 5 minutes in a Coplin jar and dipped in 0.5 Eosin Y (Sigma-Aldrich, E4009) for 12 times. The sections were dipped in distilled water until the eosin stopped streaking and successively moved through increasing concentrations of EtOH. (dipped 10 times each in 50% and 70% EtOH and equilibrated in 95% EtOH for 30 seconds and 100% EtOH for 1 minute). Xylene was used to replace the absolute alcohol and DPX (VWR, 360294H) was used for mounting. Digital images were obtained using a ZEISS Axiophot microscope with a 5x objective.

**Single MII oocyte ATP measurement**

Three weeks old *Hira*$^{f/f}$ or *Hira*$^{f/f}$ *GDF9-Cre*$^{+}$ siblings were superovulated and the cumulus-oocyte complexes were disassociated by hyaluronidase digestion. Single cell ATP measurement was conducted using ATPlite Luminescence Assay System (PerkinElmer) according to manufacturer's instructions.

**Single cell RNA-Seq on *Hira*$^{f/f}$ , *Hira*$^{f/f}$, *GDF9-Cre*$^{+}$ and *Hira*$^{f/f}$, *Zp3-Cre*$^{+}$ MII oocytes**

cDNA synthesis and amplification was performed directly on single *Hira*$^{f/f}$ , *Hira*$^{f/f}$ *Gdf9-Cre*$^{+}$ and *Hira*$^{f/f}$, *Zp3-Cre*$^{+}$ MII oocytes with the SMARTer Ultra Low Input RNA kit (Clontech). 0.5 uL of ERCC RNA spike-in mix 1 (Life Technologies), diluted 1:10$^{5}$, was

added to each reaction prior to cDNA synthesis. The amplified cDNA was fragmented by Covaris S2 sonicator (Covaris) and converted to sequencing libraries following the NEBNext DNA Library Prep (NEB) using the NEBNext Multiplex Oligos for Illumina (NEB). Bar-coded libraries were pooled and sequenced on two lanes of the Illumina HiSeq 2000 instrument. mRNA-seq reads were aligned to the mouse genome (mm9, NCBI build 37) with Bowtie v0.12.8/Tophat v2.0.2 (http://tophat.cbcb.umd.edu), which allows mapping across splice sites by reads segmentation. Annotations from Ensembl Gene version 67 were used as gene model with Tophat. Spike-in reads were aligned to ERCC spike-in sequences using bowtie2 with the following settings: -D 20 -R 3 -N 0 -L 20 -i S,1,0.50. For differential expression analysis, read counts per annotated gene were computed using HTSeq and expression level of each gene was quantified with FPKM (*Fragments Per Kilobase of Exon Per Million Fragments Mapped*) using R script. Differential expression analysis was performed using edgeR (version 3.1.10) and genes that showed significant differences at FDR < 0.1 between *Hira*$^{f/f}$ and *Hira*$^{f/f}$ *Gdf9-Cre*$^{+}$ (or between *Hira*$^{f/f}$ and *Hira*$^{f/f}$ *Zp3-Cre*$^{+}$) oocytes were identified. Gene ontology analysis of differentially expressed genes was performed with DAVID (http://david.abcc.ncifcrf.gov). For Gene Set Enrichment Analysis (version 2.0.7), the gene list was ranked based on the FDR (i.e. '1 – FDR') and fold-change (i.e. up-regulated genes were multiplied by a factor of '1'; down-regulated genes were multiplied by a factor of '-1') computed from edgeR differential expression analysis. To compare the gene expression changes between *Hira*$^{f/f}$ and *Hira*$^{f/f}$ *Gdf9-Cre*$^{+}$ (or between *Hira*$^{f/f}$ and *Hira*$^{f/f}$ *Zp3-Cre*$^{+}$) oocytes with expression changes over the course of oocyte development, we clustered previously published microarray expression data from primordial, primary, secondary, small antral and large antral follicle stages (Pan et al., 2005) using k-means clustering (n=8) and created a gene set for each cluster. Where multiple probes aligned to a single annotated gene, the mean expression value was used. For all tests, GSEA was carried out with default setting,

with the exception that the maximum gene set size was increased to 3000 genes. To determine the novel transcribed fragments that mapped entirely to intronic and intergenic regions of the mouse genome, mRNA-Seq reads were re-analysed with CuffCompare (version 2.1.1), which allows for the identification and classification of previously unannotated transcripts (Trapnell et al., 2010). The Gene Expression Omnibus (GEO) accession number for the *Hira*$^{f/f}$ *Gdf9-Cre*$^{+}$ and *Hira*$^{f/f}$, *Zp3-Cre*$^{+}$ single oocyte RNA-sequencing data is GSE66931 and GSE73382, respectively.

**Single cell whole genome bisulphite sequencing and analysis on *Hira*$^{f/f}$ and *Hira*$^{f/f}$, *Gdf9-Cre* oocytes**

To profile the DNA methylation landscape of *Hira*$^{f/f}$ and *Hira*$^{f/f}$, *Gdf9-Cre*$^{+}$ oocytes, we used a single cell bisulphite sequencing approach (scBS-Seq) that we had previously described (Smallwood et al., 2014). Briefly, MII oocytes were individually collected by mouth pipetting and lysed in a buffer containing 10mM Tris-Cl (pH 7.4), 1% SDS and 4U of Proteinase K. Bisulphite treatment was performed directly on the lysate using the Imprint DNA Modification kit (Sigma) (two-step protocol, incubation at 65 °C for 90 min, 95 °C for 3 min and 65 °C for 20 min), followed by depurination and purification of converted DNA using the PureLink PCR Micro kit (Life Technologies). First complementary strand synthesis was performed using Klenow exo- (50U, Sigma) and a biotinylated Illumina-based adapter with 9 random nucleotides for priming (biotin-CTACACGACGCTCTTCCGATCTNNNNNNNNN). This step was repeated an additional 4 times, with DNA denaturation (95 °C, 1min) in between. After capture of the neo-synthesised strands using streptavidin magnetic beads, second strand synthesis was performed using an Illumina-based adapter with 9 random nucleotides (TGCTGAACCGCTCTTCCGATCTNNNNNNNNN). Libraries were then amplified for 13 cycles using KAPA HiFi HotStart DNA Polymerase (KAPA Biosystems), Illumina PE1.0 oligo, and iPCR tag reverse oligos for indexing (Smallwood et al., 2014).

Libraries were purified using 0.8x AMPure XP beads (Agencourt) according to the manufacturer's guideline.

Libraries were assessed for quality and quantity using the Bioanalyser platform (Agilent) and the KAPA Library Quantification kit (KAPA Biosystems). For each genotype, 14 single cell libraries were pooled for sequencing (100-bp paired-end, HiSeq2500 rapid-run mode). Mapping of sequencing reads (NCBI37) and cytosine methylation extraction were performed using Bismark as previously described (Smallwood et al., 2014). The DNA methylation landscape of *Hira*$^{f/f}$ and *Hira*$^{f/f}$, *Gdf9-Cre*$^{+}$ oocytes were generated by merging all datasets from each genotype, as previously described (Smallwood et al., 2014). Data visualization and analysis were performed using SeqMonk, custom R and Java scripts.

For absolute DNA methylation quantification at the genome level or depending on the genomic contexts, individual cytosines (CpGs) were quantified (5reads cut-off). For intragenic, intergenic, exonic and intronic genomic contexts (Figure 6F), CpGs overlapping CpG islands were discarded. Promoters were defined by the genomic region (-1kbp, +200bp) surrounding annotated transcription start-sites, and CpG poor promoters were defined as promoters not overlapping CpG islands. For correlation with published oocytes whole genome bisulfite sequencing data (Shirane et al., 2013) (Figure 6C, S7E, S7I, DNA Data Bank of Japan accession number DRA000570), and for correlation with transcription, 3kb overlapping windows (1.5kb steps) were quantified for absolute level of methylation (probes defined as informative if at least 3 reads per CpGs and 7 informative CpGs per window). CGI methylation (including imprinted gDMRs) was determined by averaging individual CpGs (CpGs present in at least half of the single cells, and at least 5CpGs per CGI). The Gene Expression Omnibus (GEO) accession number for the *Hira*$^{f/f}$ and *Hira*$^{f/f}$ *Gdf9-Cre*$^{+}$ single cell bisulphite sequencing data is GSE66629.

**Detection of 5-methylcytosine by ultra-sensitive LC-MS**

Genomic DNA from oocytes was extracted using ZR-Duet DNA/RNA Miniprep kit (Zymo Reasearch) following manufacturer instructions and eluted in LC/MS grade water. DNA was digested to nucleosides using a digestion enzyme mix provided by NEB. A dilution-series made with known amounts of synthetic nucleosides and the digested DNA were spiked with a similar amount of isotope-labelled nucleosides (provided by T. Carell, LMU Munich) and separated on an Agilent RRHD Eclipse Plus C18 2.1 × 100 mm 1.8u column by using the UHPLC 1290 system (Agilent) and an Agilent 6490 triple quadrupole mass spectrometer. To calculate the quantity of individual nucleosides, standard curves representing the ratio of unlabelled over isotope-labelled nucleosides were generated and used to convert the peak-area values to corresponding quantity. Threshold for quantification is a signal-to-noise (calculated with a peak-to-peak method) above 10.

## Supplemental References

de Vries, W.N., Binns, L.T., Fancher, K.S., Dean, J., Moore, R., Kemler, R., and Knowles, B.B. (2000). Expression of Cre recombinase in mouse oocytes: A means to study maternal effect genes. Genesis *26*, 110-112.

Hajkova, P., Jeffries, S.J., Lee, C., Miller, N., Jackson, S.P., and Surani, M.A. (2010). Genome-wide reprogramming in the mouse germ line entails the base excision repair pathway. Science *329*, 78-82.

Haueter, S., Kawasumi, M., Asner, I., Brykczynska, U., Cinelli, P., Moisyadi, S., Burki, K., Peters, A.H., and Pelczar, P. (2010). Genetic vasectomy-overexpression of Prm1-EGFP fusion protein in elongating spermatids causes dominant male sterility in mice. Genesis *48*, 151-160.

Lan, Z.J., Xu, X., and Cooney, A.J. (2004). Differential oocyte-specific expression of Cre recombinase activity in GDF-9-iCre, Zp3cre, and Msx2Cre transgenic mice. Biol Reprod *71*, 1469-1474.

Nashun, B., Yukawa, M., Liu, H., Akiyama, T., and Aoki, F. (2010). Changes in the nuclear deposition of histone H2A variants during pre-implantation development in mice. Development *137*, 3785-3794.

Pan, H., O'Brien M, J., Wigglesworth, K., Eppig, J.J., and Schultz, R.M. (2005). Transcript profiling during mouse oocyte development and the effect of gonadotropin priming and development in vitro. Dev Biol *286*, 493-506.

Shirane, K., Toh, H., Kobayashi, H., Miura, F., Chiba, H., Ito, T., Kono, T., and Sasaki, H. (2013). Mouse Oocyte Methylomes at Base Resolution Reveal Genome-Wide Accumulation of Non-CpG Methylation and Role of DNA Methyltransferases. PLoS Genet *9*.

Smallwood, S.A., Lee, H.J., Angermueller, C., Krueger, F., Saadeh, H., Peet, J., Andrews, S.R., Stegle, O., Reik, W., and Kelsey, G. (2014). Single-cell genome-wide bisulfite sequencing for assessing epigenetic heterogeneity. Nat Methods *11*, 817-820.

Trapnell, C., Williams, B.A., Pertea, G., Mortazavi, A., Kwan, G., van Baren, M.J., Salzberg, S.L., Wold, B.J., and Pachter, L. (2010). Transcript assembly and quantification by RNA-Seq reveals unannotated transcripts and isoform switching during cell differentiation. Nat Biotechnol *28*, 511-515.